EX VIVO BREAST TISSUE IMAGING AND CHARACTERIZATION USING ACOUSTIC MICROSCOPY

I. Bruno, R.E. Kumon, B. Heartwell, E. Maeva, R.Gr. Maev
Centre for Imaging Research and Advanced Materials Characterization, Department of Physics, University of Windsor, 401 Sunset Ave., Windsor, Ontario N9B 3P4, Canada; ¸Hôtel-Dieu Grace Hospital, 1030 Ouellette Ave., Windsor, Ontario N9A 1E1, Canada

Abstract: As part of a pilot project, roughly-cut slices of ductal carcinoma from human mastectomies were imaged using acoustic microscopy in the range 15 to 50 MHz. C-scan images of the 2 to 5 mm thick specimens were shown to correlate well with corresponding optical images and showed higher contrast. By selective gating, internal structures could be highlighted in C-scan images that were not visible from the surfaces of the slice. Velocity and attenuation image maps of the sample were also made and then used to try to identify the tumor regions based quantitative criteria. Our results suggest that acoustic microscopy shows promise as an adjunctive method for pathologists to rapidly measure tumor size and resection margin status during intraoperative consultation and provide more complete specimen assessment during gross examination

Key words: acoustic microscopy; breast cancer; ductal carcinoma; tissue characterization

1. INTRODUCTION

At the time of surgery, surgeons sometimes have difficulty determining if they have achieved an adequate margin of normal tissue around an excised tumor. Currently, it often takes a day or more for pathologists to determine margin status via the creation of permanent sections and examination of these sections by optical microscopy. Frozen sections may be rapidly attained, but can exhibit undesirable image artifacts and are contraindicated for small lesions and some pathologies. Hence a method to accurately and rapidly determine margin status on arbitrary unfixed tissue at the time of

M.P. André (ed.), Acoustical Imaging, 279–287.

surgery would reduce re-operative rates, patient anxiety, and local recurrence rates and free up limited resources.

Acoustic microscopy has the potential to provide pathologists an adjunctive method to allow determination of tumor dimensions and the width of resection margins on gross specimens at the time of initial surgery and during subsequent gross examination. It can be performed without any special sample preparation on both unfixed and fixed tissue and yet still achieve high contrast imaging. Without the need for dehydration and paraffin-embedding, acoustic microscopy is able to provide images of tissue closer to its native state, while still achieving sub-millimeter to micron-scale resolution. Finally, it can detect sub-surface features throughout the volume of optically opaque tissue even when the specimen has macroscopically large dimensions (mm or cm) and thus provide more thorough specimen sampling than thin sampling of permanent sections will allow.

Among breast cancers, ductal carcinoma is the most common type. Its characteristics relevant to ultrasound include a solid core, indurations, comedo necrosis, above-normal density and collagen content, and sometimes clustered micro-calcifications[1]. These parameters influence ultrasound reflection and propagation, resulting in visualization of tumor boundaries with diagnostic ultrasound[2]. Early studies using 600 MHz transmission acoustic microscopy demonstrated normal and diseased tissue could be distinguished[3]. Studies have also been performed to measure the velocity[4–8], attenuation[5–10], and backscatter coefficient[5,6,8,11–13] of normal, benign, and malignant breast tissue both *in vivo* and *ex vivo*, although all of these measurements were done in the diagnostic ultrasound frequency range (1 to 13 MHz). Foster et al.[5,6] used a scanning acoustic microscope at 3 to 7 MHz and 13 MHz to produce images and make quantitative measurements of thick breast tissue specimens. While they found that malignant tissue could be distinguished from other tissue based on ultrasound measurements, their results also suggest that the distinction could be enhanced at higher frequencies, particularly with respect to attenuation and backscatter. In light of the literature discussed above, we anticipated noticeable differences between cancerous and healthy tissue in images obtained with an acoustic microscope at frequencies of 15 MHz and above. This work extends our group's recent research on acoustical characterization of skeletal and dental tissue[14,15] into the soft tissue domain[16,17].

2. EXPERIMENT AND THEORY

Specimens of human breast tissue were investigated using acoustic microscopy in the frequency range 15 to 50 MHz. Imaging was performed in

reflection mode using Sonix HS-1000 and Tessonics AM1103 scanning acoustic microscopes. The hardware and software for the latter device were custom-designed at our center. Roughly-cut samples from a mastectomy were examined, each of which was approximately 2 x 2 cm in size and 2 to 5 mm thick. The specimens were fixed in formalin and never frozen. All samples were immersed in degassed water at room temperature during imaging. A plastic plate was secured on top of the sample to minimize scattering due to surface topography, and a glass plate was used in some cases as a substrate to increase the amount of reflected signal. The transducer was raster-scanned over the specimen and the resulting A-scan data was recorded at every point. B-scan and C-scan images could then be constructed by assigning grayscale values to the appropriately-gated sections of the A-scan data.

To generate quantitative image maps of velocity and attenuation, an insertion method was employed, whereby the properties of the tissue are computed in reference to a position without tissue (i.e., only water). For the purposes of the calculations, the acoustic beam is assumed to be planar throughout the specimen. Point-to-point variations in the sample thickness were accounted for by computing the distance between the top and bottom plates, assuming the bottom plate is flat. In the case where the bottom plate is level, the velocity at position (x, y) is then given by

$$c(x,y) = \frac{2L(x,y)}{t_s(x,y) - t_c(x,y)} = \frac{t_s^0 - t_c(x,y)}{t_s(x,y) - t_c(x,y)} c_0 \,, \tag{1}$$

where L is the distance between the bottom of the cover plate and top of the substrate, t_s and t_c are the signal travel times to the tissue-substrate and cover-tissue interfaces, respectively, t_s^0 is the travel time to the cover-water interface at the reference point, and c_0 is the velocity of the water. The attenuation in decibels per unit length is given at each position by

$$\alpha_{\bar{v}}(x,y) = \frac{-20}{2L(x,y)} \log_{10}\left[\frac{A(x,y)}{A_0}\right], \tag{2}$$

where A and A_0 are the peak amplitudes of the signal after passing through the specimen and water reference locations, respectively. Note that this equation does not account for frequency-dependent effects, and therefore is essentially an estimate of the attenuation at the center frequency of the transducer.

3. RESULTS AND DISCUSSION

To begin, a qualitative study of the specimens was performed. Figure 1 shows a comparison of optical (Fig. 1a) and acoustical images (Fig. 1b) of Specimen I. The acoustical C-scan image is produced using a 25 MHz focused transducer focused at the bottom of the sample. While the carcinoma can be seen in the optical image (lighter shade of gray; in color it is typically white while the surrounding tissue is flesh-colored), the acoustical image exhibits higher contrast and shows more of the sub-surface tissue structure. The black and white arrows in the images point to common regions where the carcinoma is branching into the surrounding margin. In addition, the acoustical image clearly shows a clear dark band starting near the vertical gray arrow and proceeding around the tumor and corresponds to a yellow band surrounding the tumor in the optical image. Figure 2 shows images of Specimen II and provides an example of placing the transducer focus at the top and bottom of the sample. In the former case (Fig. 2a), the reflected signal is primarily a function of the reflection coefficient at the cover-tissue interface and thus represents an image of the local acoustic impedance. The higher acoustic impedance of the tumor is indicative of higher density, higher velocity, or both. In the latter case (Fig. 2b), the image is primarily a function of the round-trip attenuation of the signal as it passes through the specimen. In contrast to Fig. 1b, a distinct border of higher attenuation is observed around the perimeter of the tumor, not just at some distance around it. This result may be in part due to the fact that a plastic substrate was used in Fig. 2(b).

Because changes in tissue velocity cause the received signals to arrive at slightly different times, different regions of the specimen can be selectively displayed by narrowly gating the A-scan data. Figure 3 shows C-scan images produced from a single scan of Specimen II using the Tessonics microscope at 50 MHz with the focus of the transducer placed at the tissue-glass interface. These images highlight (Fig. 3a) the tumor margin as well as thin extensions of the tumor extending into the surrounding tissue, (Fig. 3b) the main body of the carcinoma, and (Fig. 3c) a sinuous structure, possibly a microvessel. The latter feature was not visible from the surface and appears when the specimen is imaged from either side, suggesting that it is internal to the volume of the slice.

Next, quantitative measurements of the velocity and attenuation were calculated at each scan point using the method described in Sec. 3 for Specimen II but using the Tessonics microscope. Figure 4 shows an image map of the velocity as a function of position and a corresponding histogram of the measured values. The measurements show two major peaks in ranges 1480–1485 m/s, corresponding to the water, and 1550–1570 m/s, corresponding to the tumor. The latter range is in line with previous velocity

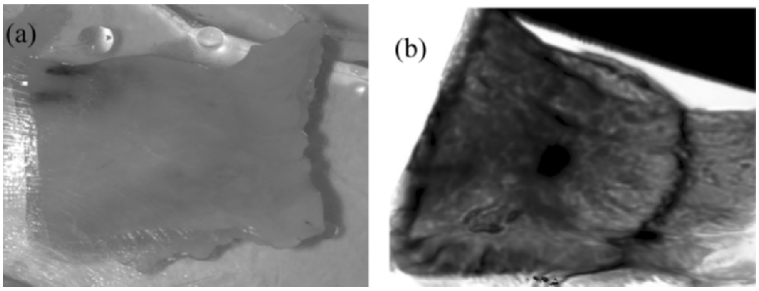

Figure 1. Comparison of (a) optical and (b) acoustical images of a ductal carcinoma**.** The optical image is not stained. The acoustical image was produced at 25 MHz using the Sonix microscope with the transducer focused on the back side of the 4 mm thick, roughly-cut slice and a glass substrate (the acoustical image is slightly stretched horizontally). The arrows point to common features, as described in the text.

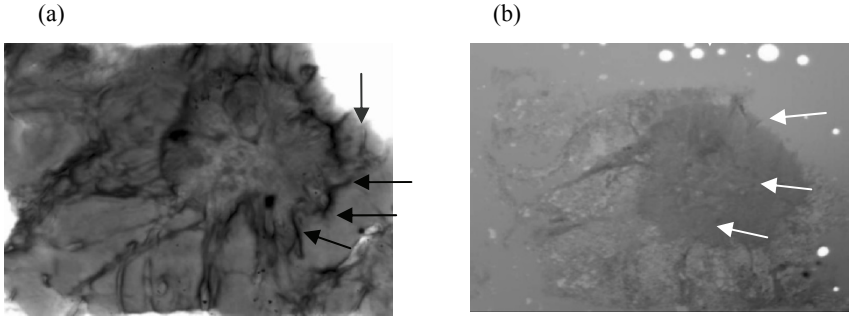

Figure 2. Acoustical images of a ductal carcinoma with transducer focused on the (a) top and (b) bottom of the specimen. These images were produced on an approximately 2 mm thick specimen using the Sonix microscope with a 50 MHz transducer and plastic substrate.

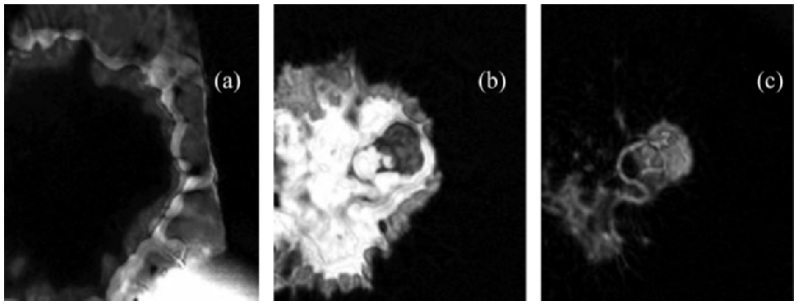

Figure 3. Examples of acoustical images created by gating A-scan data to highlight (a) margin, (b) tumor, and (c) an internal feature. All three images were created from the data obtained from a single scan of the Tessonics microscope for the same specimen as in Fig. 2.

measurements of breast carcinoma[5,7]. Figure 5 shows an image map of the attenuation. (The white spots inside the tissue image correspond to regions where small bubbles were trapped on top of the specimen thereby preventing meaningful attenuation measurements in those regions.) The attenuation of the carcinoma at 50 MHz is seen to be significantly lower than the surrounding tissue. This result is qualitatively consistent with previous measurements in the diagnostic ultrasound frequency range (5–13 MHz)[5–10], although the measured values are less than what might be expected by simple extrapolation from these previous measurements.

To determine if the velocity and attenuation data from Figures 4 and 5 could be combined to identify regions of abnormal tissue development, a two-dimensional histogram was constructed, as shown in Fig. 6a, where the grayscale is proportional to the area corresponding to each (c, α) pair. The rectangular regions drawn on the histogram are two subsets of the velocity and attenuation data: (1) 1550–1590 m/s and 0 to 1 dB/mm, enclosed by the gray rectangle, and (2) 1500–1590 m/s and 0 to 2 dB/mm, enclosed by the black rectangle. The image regions corresponding to these parameter subsets were then marked with corresponding colors on the C-scan of Fig. 6b, with the result shown in Fig. 6(c). (Fig. 6b is a C-scan image generated from the same data set as in Figure 3). The gray region, corresponding approximately to the range of velocity values found in the literature for breast carcinoma[4–8], appears to underestimate the extent of the tumor, whereas the larger black region seems to identify the tumor region better. This type of approach could be useful for computerized sizing of tumors and/or margins, a desired capability for pathological assessment. For example, the areas of the gray and black marked regions in Fig. 6c were computed to be 27 mm^2 and 49 mm^2, with equivalent circular diameters of 6 mm and 8 mm, respectively.

4. CONCLUSION

Our pilot study has examined the use of acoustic microscopy in the range of 15 to 50 MHz to image ductal carcinoma specimens up to 5 mm in thickness. Although these results are promising, additional work needs to be done to make acoustic microscopy a robust and reliable tool for gross tissue examination in the pathology laboratory. Future efforts will include a detailed analysis of the specimen pathology via permanent sections, examination of additional fixed and unfixed specimens with different kinds of benign and malignant lesions, and measurement of acoustical backscatter.

This project was supported by the Canadian Institutes of Health Research (CIHR) and the Natural Science and Engineering Research Council (NSERC) of Canada.

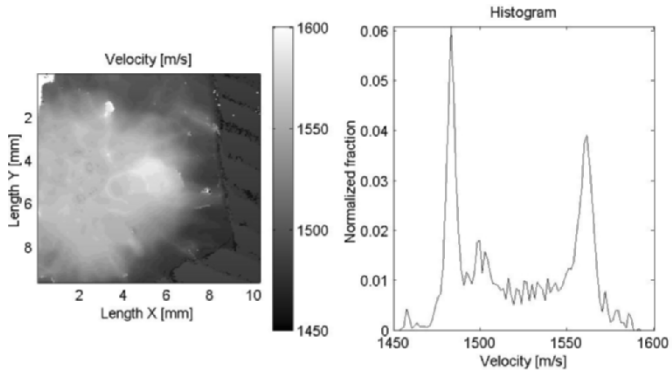

Figure 4. Image map of velocity data for ductal carcinoma and corresponding distribution of measured values**.** The tumor has noticeably higher velocity than the surrounding tissue. In Fig. 6, this data is combined with attenuation measurements of Fig. 5.

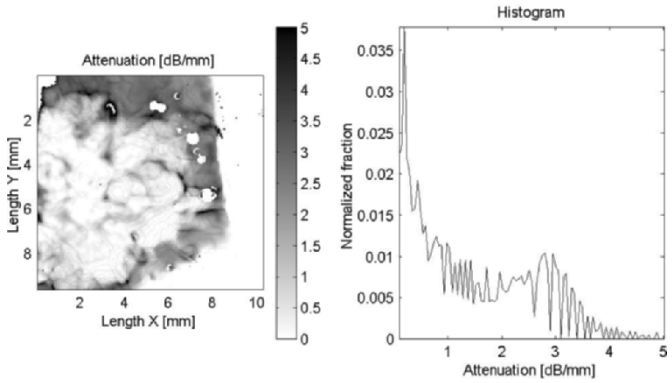

Figure 5. Image map of attenuation data for ductal carcinoma and corresponding distribution of measure values. The tumor has noticeably lower attenuation than the surrounding tissue. In Fig. 6, this data is combined with the velocity measurements of Fig. 4.

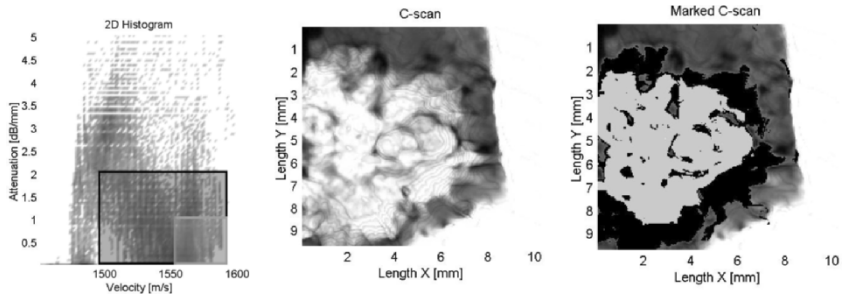

Figure 6. C-scan marking using quantitative data analysis**.** The figure shows (a) a two-dimensional histogram of velocity and attenuation data, (b) an unmarked C-scan image, and (c) a marked C-scan image. The parameter subsets enclosed by the gray and black rectangles in the histogram (a) correspond with the gray and black regions marked in image (c).

REFERENCES

1. M.E. Anderson, M.S. Soo, R.C. Bentley, and G.E. Trahey, The detection of breast micro-calcifications with medical ultrasound, *J. Acoust. Soc. Amer.* **101**, 29–39 (1997).
2. M.P. André, M. Galperin, L.K. Olson, K. Richman, S. Payrovi, and P. Phan, Improving the accuracy of diagnostic breast ultrasound in: *Acoustical Imaging, v. 26,* edited by R.Gr. Maev (Kluwer Academic/Plenum Press, New York, 2002), pp. 453–460,.
3. R.A. Lemons and C.F. Quate, Acoustic microscopy: Biomedical application, *Science* **188**, 905–914 (1975).
4. G. Kossoff, E.K. Fry, and J. Jellins, Average velocity of ultrasound in the human female breast, *J. Acoust. Soc. Am.* **53**, 1730–1736 (1973).
5. F.S. Foster, M. Strban, and G. Austin, The ultrasound macroscope: Initial studies of breast tissue, *Ultrasonic Imaging* **6**, 243–261 (1984).
6. F.T. D'Astous, and F.S. Foster, Frequency dependence of ultrasound attenuation and backscatter in breast tissue, *Ultrasound Med. Biol.* **12**, 795–808 (1986).
7. P.D. Edmonds, C.L. Mortensen, J.R. Hill, S.K. Holland, J.F. Jensen, P. Schattner, A.D. Valdes, R.H. Lee, and F.A. Marzoni, Ultrasound tissue characterization of breast biopsy specimens, *Ultrasonic Imaging* **13**, 162–185 (1991).
8. C.L. Mortensen, P.D. Edmonds, Y. Gorfu, J.R. Hill, J.F. Jensen, P. Schattner, L.A. Shifrin, A.D. Valdes, S.S. Jeffrey, and L.J. Esserman, Ultrasound tissue characterization of breast biopsy specimens: Expanded study, *Ultrasonic Imaging* **18**, 215–230 (1996).
9. C. Calderon, D. Vilkomerson, R. Mezrich, K.F. Etzold, and M. Haskin, Differences in the attenuation of ultrasound by normal benign and malignant breast tissue, *J. Clin. Ultrasound* **4**, 249–254 (1976).
10. E. Kelly Fry, N.T. Sanghvi, and F.J. Fry, Frequency dependent attenuation of malignant breast tumors studied by the fast Fourier transform technique, in: *Ultrasonic Tissue Characterization II, NBS Spec. Publ. 525,* edited by M. Linzer (U.S. Government Printing Office, Washington, DC, 1979), pp. 85–91.
11. R.M. Golub, R.E. Parsons, B. Sigel, E.J. Feleppa, J. Justin, H.A. Zaren, M. Rorke, J. Sokil-Melgar, and H. Kimitsuki, Differentiation of breast tumors by ultrasonic tissue characterization, *J. Ultrasound Med.* **12**, 601–608 (1993).

12. T.M. Burke, T.A. Blankenberg, A.K.Q. Siu, F.G. Blankenberg, and H.M. Jensen, Preliminary investigation of ultrasound scattering analysis to identify women at risk for later invasive cancer, *Ultrasound Med. Biol.* **21**, 295–303 and 305–311 (1995).
13. M.E. Anderson, M.S.C. Soo, and G.E. Trahey, In vivo breast tissue backscatter measurements with 7.5- and 10-MHz transducers, *Ultrasound Med. Biol.* **27**, 75–81 (2001).
14. L.A. Denisova, R.Gr. Maev, I.V. Matveichuk, Yu.I. Denisov-Nikolsky, A.A. Denisov, and E.Yu. Maeva, Investigating bone microstructure and mechanical properties using acoustic microscopy in: *Acoustic Imaging, v. 26,* edited by R. Gr. Maev (Kluwer Academic/Plenum Press, New York, 2002), pp. 61–68.
15. R. Maev, L. Denisova, E. Maeva, and A. Denissov, New data on histology and physico mechanical properties of human tooth tissue obtained with acoustic microscopy, *Ultrasound Med. Biol.* **28**, 131–136 (2002).
16. E. Maeva, I. Bruno, M. Docker, B. Zielinsky, F. Severin, and R.Gr. Maev, Method of acoustic microscopy for sex determination of sea lamprey, petromyzon marinus larvae, *J. Fish Biol.* **65**, 148–156 (2004).
17. R.E. Kumon, I. Bruno, B. Heartwell, and E. Maeva, Breast tissue characterization with high-frequency scanning acoustic microscopy, *J. Acoust. Soc. Am.* **115**, 2376(A) (2004).